Optics Letters

Adjustment-free two-sided 3D direct laser writing for aligned micro-optics on both substrate sides

Michael Schmid,[1,*] Simon Thiele,[2] Alois Herkommer,[2] and Harald Giessen[2]

[1]4th Physics Institute and Research Center SCoPE, University of Stuttgart, Pfaffenwaldring 57, 70569 Stuttgart, Germany
[2]Institute of Applied Optics (ITO) and Research Center SCoPE, University of Stuttgart, Pfaffenwaldring 9, 70569 Stuttgart, Germany
*Corresponding author: m.schmid@pi4.uni-stuttgart.de

Received 26 September 2022; revised 3 November 2022; accepted 11 November 2022; posted 15 November 2022; published 22 December 2022

3D direct laser writing is a powerful and widely used tool to create complex micro-optics. The fabrication method offers two different writing modes. During the immersion mode, an immersion medium is applied between the objective and the substrate while the photoresist is exposed on its back side. Alternatively, when using the dip-in mode, the objective is in direct contact with the photoresist and the structure is fabricated on the objective facing side of the substrate. In this Letter, we demonstrate the combination of dip-in and photoresist immersion printing, by using the photoresist itself as immersion medium. This way, two parts of a doublet objective can be fabricated on the front and back sides of a substrate, using it as a spacer with a lateral registration below 1 µm and without the need of additional alignment. This approach also enables the alignment free combination of different photoresists on the back and front sides. We use this benefit by printing a black aperture on the back of the substrate, while the objective lens is printed on the front. © 2022 Optica Publishing Group

https://doi.org/10.1364/OL.476448

Since its introduction in 1997 [1], multiphoton 3D direct laser writing has greatly improved. The fabrication method uses a high intensity fs-pulsed laser beam that is focused into a photoresist which leads to two- or multi-photon absorption in the focal region and thus triggers polymerization and hardening. By moving the focal spot relative to the substrate, arbitrary three-dimensional structures can be created. Early on, immersion fluids were used to mediate contact between the objective and the substrate. Dip-in laser lithography was introduced subsequently, using the photoresist itself as immersion medium [2]. This fabrication method removed the height restriction of immersion writing and simplified the fabrication process [3]. Other writing modes overcoming height restrictions were introduced, such as WOW-2PP [4]. Since then, direct laser writing has been used to create a variety of different complex microstructures and micro-optics in different scientific fields such as imaging [5], optical communication [6,7], sensing [8–10], or trapping [11,12]. Furthermore, the complexity of 3D printed optics increased drastically over time by developing new optical designs like multi-lens objectives [13,14] or new photoresists with different dispersion and their combination [15–19].

However, all of the mentioned 3D printed micro-optics are always fabricated on the same side of the used substrate, since writing on both sides of the sample would require development, flipping, and reinserting the substrate into the fabrication system.

Here, we simplify this process dramatically by using a combination of the immersion and dip-in methods. Thus, it is possible to print on both sides of a substrate in a single fabrication step without the need to develop and flip the sample in-between, and with great registration accuracy. The writing process is illustrated in Fig. 1. In the first step, the structure on the distant side of the substrate is printed through it, with the photoresist being the immersion medium between objective and the near side of the substrate. Therefore, a droplet of the photoresist is also put onto the distant side of the substrate. Within that droplet, the structure is being fabricated. After the fabrication, the objective is moved along the propagation axis to align the focal spot with the near side of the substrate. In a second step, the structure on the near side of the substrate is printed in dip-in configuration without any adjustment required. The photoresist between the objective and the near side of the substrate which acted as an immersion medium for the print on the back side serves now also the medium to be polymerized.

In both cases, the fabrication is initiated at the substrate to have good adhesion of the structure and to avoid the need for supporting structures. Since the structure on the back side is fabricated first, it does not intervene with the beam path during the fabrication of the second structure.

This fabrication process offers the possibility to fabricate structures on both sides of a substrate without the need to develop and flip the sample in-between the writing processes and therefore offers a high accuracy without the need for additional markers or alignment. To quantify the residual lateral displacement, we fabricate markers on both sides of a 170-µm- and 540-µm-thick D263 substrate without moving the piezo stage in between. We fabricate the structures using a Nanoscribe Photonic Professional GT (Nanoscribe GmbH, Germany) direct laser writing machine with the photoresist IP-S from Nanoscribe. We image the resulting structures with an optical microscope (Keyence VHX-6000) and depict the images for the 170-µm substrate in Fig. 2. Under a viewing angle of

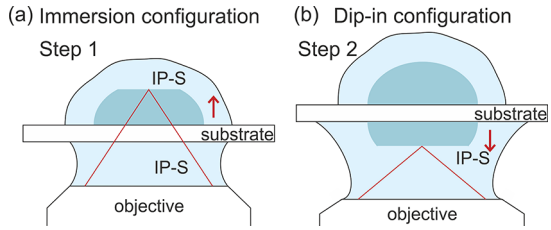

Fig. 1. Sketch of the writing process. (a) Structure on the distant side of the substrate is printed through it, with the photoresist being the immersion medium. (b) After that, the structure on the near side of the substrate is printed in dip-in configuration without any adjustment required. In both cases, one starts the fabrication at the substrate to have good adhesion of the structure.

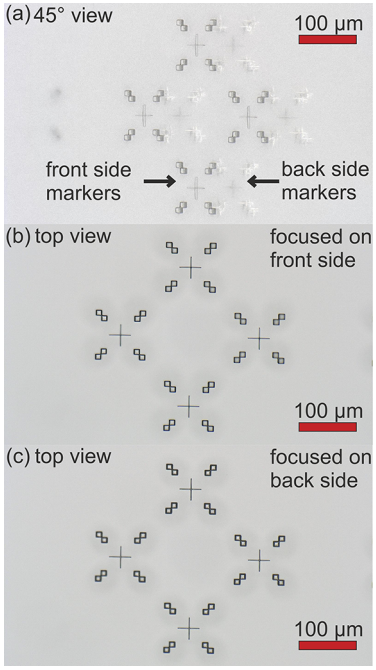

Fig. 2. Markers printed on both sides of a 170-µm-thick substrate to quantify the lateral displacement. (a) A 45° angled view images the structures on the front and back sides simultaneously. Top views focused on the (b) front side and the (c) back side without moving the sample in between visualize the resulting displacement below 1 µm which is small enough for the creation of two-sided optical designs.

45°, the markers on the front and the back side are both visible. We also take images with the top view and focus on the front and back side, respectively. Between the measurements, the microscope does not move in the xy-plane. By comparing the marker positions in both images, we can determine the lateral displacement of the markers at 0.33 µm for the 170-µm substrate and 0.97 µm for the 540-µm substrate, which is submicron accuracy. The shift is mostly due to a small tilt angle of the substrate of 0.08° in the Nanoscribe machine. The resulting lateral shifts are small enough to enable the fabrication of optics on both sides of the substrate without the need for further alignment.

To demonstrate this capability, we fabricate an aspheric doublet objective with one lens on the back and one lens on the front of the substrate. The design and writing results are depicted in

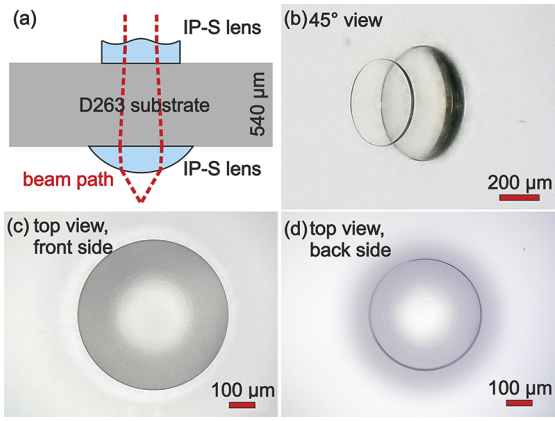

Fig. 3. Doublet objective, consisting of two aspheric lenses on both sides of the substrate. No alignment markers are required. (a) Sketch of the aspheric doublet objective design. (b) A 45° angled view on the back side shows both lenses simultaneously. Top views on the (c) front and (d) back sides depict the lenses individually.

Fig. 3. In this case, we use a 540-µm-thick D263 (Menzel) substrate to increase the distance between the two lenses which is beneficial for the optical design. The optical design is optimized using ZEMAX with aspheric surfaces on the front (near) and back (distant) lenses. For later comparison, we also design an aspheric singlet lens to compare the imaging quality. We fabricate the lens on the back side at first to avoid possible interference of the front lens with the laser beam during the printing process. Both lenses are made of the photoresist IP-S from Nanoscribe with a refractive index n_d of 1.511 in its 2PP state [20]. We use a 25× Zeiss objective (LD LCI Plan-Apochromat 25×/0.8 Imm Corr DIC M27 25×/0.8, adaptive ring positioned to match IP-S) with a long working distance of 740 µm. The long working distance is crucial to enable the printing on the back side of the 540-µm-thick glass substrate. The fabrication parameters are slicing 0.2 µm, hatching 0.5 µm, and scan speed 50 mm/s. The used laser power is 70% (average intensity of 100% is approximately 58 mW, with a repetition rate of 80 MHz, the pulse energy at 70% is 508 pJ or an intensity of 2.59 TW/cm^2) and the piezo settling time is 2 seconds. We rotate the hatching angle by 30° after each layer, for which we use the galvo scan mode. After the printing job, the sample is developed in mr-Dev 600 (20 min) to remove the residual photoresist and cleaned in isopropanol (5 min). Figure 4 depicts the confocal light microscopy measurements of the surfaces of the front and back lenses of the doublet design, as well as a comparison singlet design printed in dip-in configuration. The singlet lens and the front lens of the doublet, which are both printed in dip-in mode, show a good agreement of the surface measurements with the design, showing deviations between +/− 0.3 µm which is sufficient for the optical surface. However, the lens on the back side exhibits large deviations up to 5 µm, which are probably due to the refractive index mismatch between the substrate and IP-S in its unpolymerized liquid state ($n_d = 1.486$) influencing the laser beam path.

They could be reduced by using better matching photoresists like IP-Dip. This deviation is obviously too big for an optical surface and would strongly reduce the imaging quality. However, these big deviations can be compensated by adding the difference between the design and the measured surface profile on top of the original design and fabricate this corrected structure [5]. After

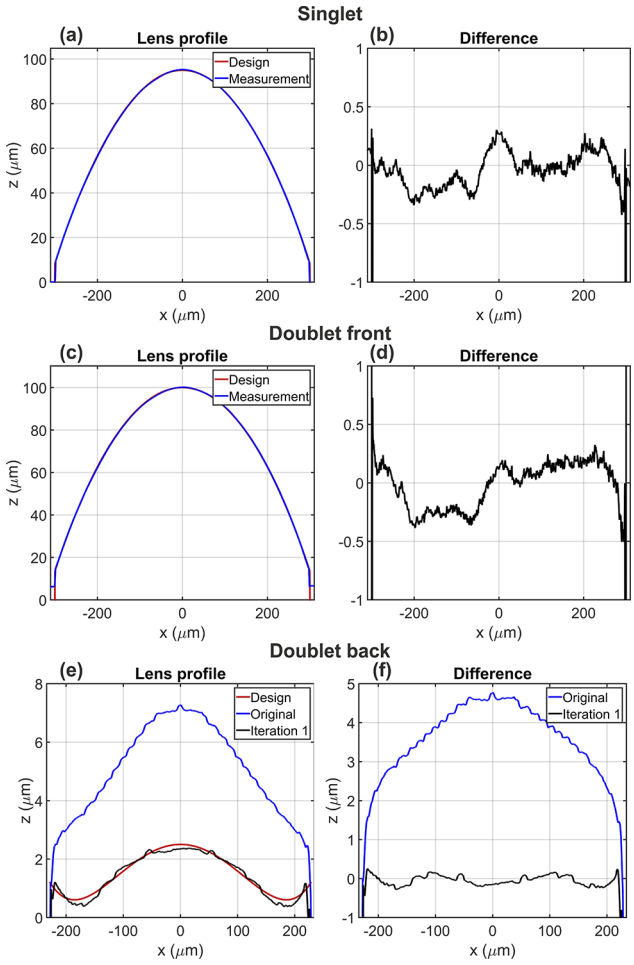

Fig. 4. Surface profile and deviation from design for (a), (b) the singlet lens, (c), (d) the front lens, and (e), (f) the back lens before and after one iteration. The deviation for the singlet lens as well as the front lens of the doublet are below +/− 0.3 μm and do not need to be corrected. However, the back lens of the doublet has strong deviations up to several μm. We correct them by adding the difference between design and measured profile to the design, and fabricate the resulting structure. After the correction, the deviations are below +/− 0.2 μm.

just one iteration, this compensation process results already in deviations below +/− 0.2 μm which is sufficient for the optical surface [Fig. 4(f)]. With the corrected back lens surface, we compare the imaging result of the aspheric singlet lens with the aspheric two-sided doublet lens by imaging an USAF 1951 resolution test target (see Fig. 5). For the imaging of the USAF test target, we use a home-built microscopy setup [5,21,22] with white light illumination. We use an LED which is collimated by an achromatic lens, illuminating a diffusor plate to ensure uniform illumination.

A Mitutoyo 10× objective is used in the setup to focus the light onto the sample. The USAF 1951 resolution test target is placed between the objective and the sample. The resulting image is viewed with a standard microscopy setup consisting of a 20× objective, a tube-lens, and a CMOS sensor. To block undesired stray light which is projected onto the back side of the substrate, we add an adjustable iris diaphragm between the diffuser plate and the objective. By adjusting the diameter of the image of the diaphragm to match the diameter of the lens, we simulate a

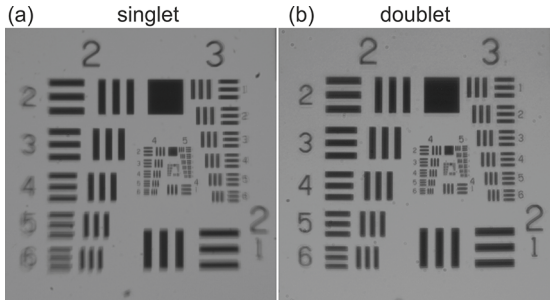

Fig. 5. Image of an USAF 1951 resolution test target with (a) the aspheric singlet reference lens and (b) the two-sided aspheric objective after surface corrections. The singlet lens shows aberrations close to the edges of the image resulting in blurring while the doublet objective is much sharper over the entire viewing field.

physical aperture. The imaging of the USAF test target with the aspheric singlet lens results in a sharp image in the center, but toward the edges, aberrations reduce the imaging performance [see Fig. 5(a)]. In the image taken with the two-sided aspheric lens, the aberrations are reduced and the image is much sharper also toward the edges, as expected. Using the substrate as spacer, a doublet objective is created without the need for supporting structures which have often been used previously [13,14]. In this case, the photoresist on the front and back sides of the substrate was the same, namely IP-S, but it is possible to use different photoresists or other 3D printable materials thus offering more design freedom, for example, for the creation of achromats or apochromats [15,16].

In Fig. 6, we demonstrate the combination of different photoresists on the front and back sides to create an aspheric singlet lens in combination with an aperture to render the projected diaphragm from the previous illumination setup redundant. On the front side of the substrate, we fabricate the same aspheric singlet lens from IP-S as before, while on the back side, we create an aperture consisting of the extremely dense black photoresist Prototype IP-Superblack. The 10-μm high aperture with an outer diameter of 800 μm and an inner diameter of 300 μm is printed with a laser power of 30% (pulse energy 218 pJ or intensity of 1.11 TW/cm^2) and a scan speed of 80 mm/s. To print this material, only the immersion configuration can be used due to the high absorption. With our new fabrication configuration, we can combine it easily with the IP-S singlet lens on top without any additional adjustments. An image of the printed aperture is displayed in Fig. 6(b). For imaging the USAF 1951 test target, we use the same setup as before, without the additional diaphragm. Comparing the imaging results of the lens with and without the printed aperture, a clear contrast improvement is visible [Figs. 6(c) and (e)].

Using an intensity comparison of a cut through of a line segment [Fig. 6(d)], it is visible that the contrast improves significantly. The Michelson contrast enhances by a factor of more than 2.

In summary, we introduced a new writing configuration using the photoresist itself as immersion medium to simultaneously print on the front and back sides of a substrate. We showed that the lateral displacement below 1 μm is good enough to create micro-optics on the front and back sides without further alignment and demonstrated the improved imaging quality of a doublet lens fabricated in this configuration. Furthermore, we demonstrated the combination of different photoresists on the

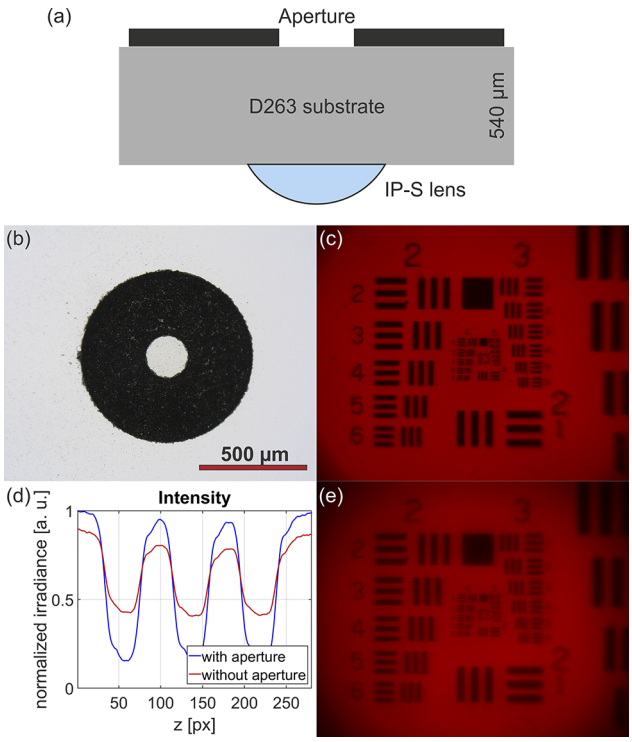

Fig. 6. (a) Imaging system consisting of a singlet lens in combination with a printed aperture on the back side of the substrate. (b) A 10-µm-thick aperture made from Prototype IP-Superblack can be printed in photoresist dip-in configuration. Imaging of an USAF 1951 test target with the singlet reference lens (c) with the aperture and (e) without the aperture reveals (d) a contrast difference by a factor of more than 2.

front and back sides of the material by combining an IP-S lens with a 3D printed aperture on the back improving the imaging contrast.

Our work paves the way toward complex, multi-resist printing, including stops and hulls directly, without the need for support structures. The combination with novel 2PP of glass [23] offers huge potential toward purely glassy environmentally durable micro-optical systems in the future.

Funding. Ministerium für Wissenschaft, Forschung und Kunst Baden-Württemberg (ICM Project 5D Printing); European Research Council (3DPRINTEDOPTICS, COMPLEXPLAS); Baden-Württemberg Stiftung (OPTERIAL); Bundesministerium für Bildung und Forschung (13N10146, PRINTFUNCTION, PRINTOPTICS); Deutsche Forschungsgemeinschaft (GRK 2642).

Acknowledgements. We thank Andrea Toulouse and Simon Ristok for help with the imaging setup and Prof. Wilhelm Stork for valuable discussions, and Gips-Schüle-Stiftung for support.

Disclosures. MS: University of Stuttgart (P), ST: University of Stuttgart (P), AH: University of Stuttgart (P), HG: University of Stuttgart (P).

Data availability. Data underlying the results presented in this paper are not publicly available at this time but may be obtained from the authors upon reasonable request.

REFERENCES

1. S. Maruo, O. Nakamura, and S. Kawata, Opt. Lett. **22**, 132 (1997).
2. T. Bückmann, N. Stenger, M. Kadic, J. Kaschke, A. Frölich, T. Kennerknecht, C. Eberl, M. Thiel, and M. Wegener, Adv. Mater. **24**, 2710 (2012).
3. A.-I. Bunea, N. d. C. Iniesta, A. Droumpali, A. E. Wetzel, E. Engay, and R. Taboryski, Micro **1**, 164 (2021).
4. K. Obata, A. El-Tamer, L. Koch, U. Hinze, and B. N. Chichkov, Light: Sci. Appl. **2**, e116 (2013).
5. S. Ristok, S. Thiele, A. Toulouse, A. M. Herkommer, and H. Giessen, Opt. Mater. Express **10**, 2370 (2020).
6. P. I. Dietrich, M. Blaicher, I. Reuter, M. Billah, T. Hoose, A. Hofmann, C. Caer, R. Dangel, B. Offrein, U. Troppenz, M. Moehrle, W. Freude, and C. Koos, Nat. Photonics **12**, 241 (2018).
7. A. Landowski, D. Zepp, S. Wingerter, G. Von Freymann, and A. Widera, APL Photonics **2**, 106102 (2017).
8. P. Dietrich, G. Göring, M. Trappen, M. Blaicher, W. Freude, T. Schimmel, H. Hölscher, and C. Koos, Small **16**, 1904695 (2020).
9. S. Rekštyte, D. Paipulas, M. Malinauskas, and V. Mizeikis, Nanotechnology **28**, 124001 (2017).
10. J. A. Kim, D. J. Wales, A. J. Thompson, G.-Z. Yang, J. A. Kim, D. J. Wales, A. J. Thompson, and G.-Z. Yang, Adv. Opt. Mater. **8**, 1901934 (2020).
11. C. Liberale, P. Minzioni, F. Bragheri, F. De Angelis, E. Di Fabrizio, and I. Cristiani, Nat. Photonics **1**, 723 (2007).
12. A. Asadollahbaik, S. Thiele, K. Weber, A. Kumar, J. Drozella, F. Sterl, A. M. Herkommer, H. Giessen, and J. Fick, ACS Photonics **7**, 88 (2020).
13. K. Weber, Z. Wang, S. Thiele, A. Herkommer, and H. Giessen, Opt. Lett. **45**, 2784 (2020).
14. T. Gissibl, S. Thiele, A. Herkommer, and H. Giessen, Nat. Photonics **10**, 554 (2016).
15. M. Schmid, S. Thiele, A. Herkommer, and H. Giessen, Opt. Lett. **43**, 5837 (2018).
16. M. Schmid, F. Sterl, S. Thiele, A. Herkommer, and H. Giessen, Opt. Lett. **46**, 2485 (2021).
17. L. Yang, F. Mayer, U. H. F. Bunz, E. Blasco, and M. Wegener, Light Adv. Manuf. **2**, 1 (2021).
18. K. Parkatzidis, M. Chatzinikolaidou, M. Kaliva, A. Bakopoulou, M. Farsari, and M. Vamvakaki, ACS Biomater. Sci. Eng. **5**, 6161 (2019).
19. D. Gailevičius, V. Padolskytė, L. Mikoliūnaitė, S. Šakirzanovas, S. Juodkazis, and M. Malinauskas, Nanoscale Horiz. **4**, 647 (2019).
20. M. Schmid, D. Ludescher, and H. Giessen, Opt. Mater. Express **9**, 4564 (2019).
21. A. Toulouse, S. Thiele, H. Giessen, and A. M. Herkommer, Opt. Lett. **43**, 5283 (2018).
22. A. Toulouse, S. Thiele, H. Giessen, and A. M. Herkommer, Semantic Scholar **10930**, 48 (2019).
23. D. Gonzalez-Hernandez, S. Varapnickas, G. Merkininkaitė, A. Čiburys, D. Gailevičius, S. Šakirzanovas, S. Juodkazis, and M. Malinauskas, Photonics **8**, 577 (2021).